Supplementary Information

AtPRMT3-RPS2B promotes ribosome biogenesis and coordinates growth and cold adaptation trade-off

Zhen Wang[1, 2, 3, #, *], Xiaofan Zhang[1, 2, #], Chunyan Liu[1], Susan Duncan[3], Runlai Hang[1], Jing Sun[1], Lilan Luo[1], Yiliang Ding[3], Xiaofeng Cao[1, 2, *]

[1] Institute of Genetics and Developmental Biology, Chinese Academy of Sciences, Beijing, 100101, China

[2] University of Chinese Academy of Sciences, Beijing, 100039, China

[3] John Innes Centre, Norwich Research Park, Norwich, NR4 7UH, United Kingdom

[#] Z.W. and X.Z. contributed equally to this work.

[*] Corresponding author: xfcao@genetics.ac.cn (X.C.) and z.wang@genetics.ac.cn (Z.W.)

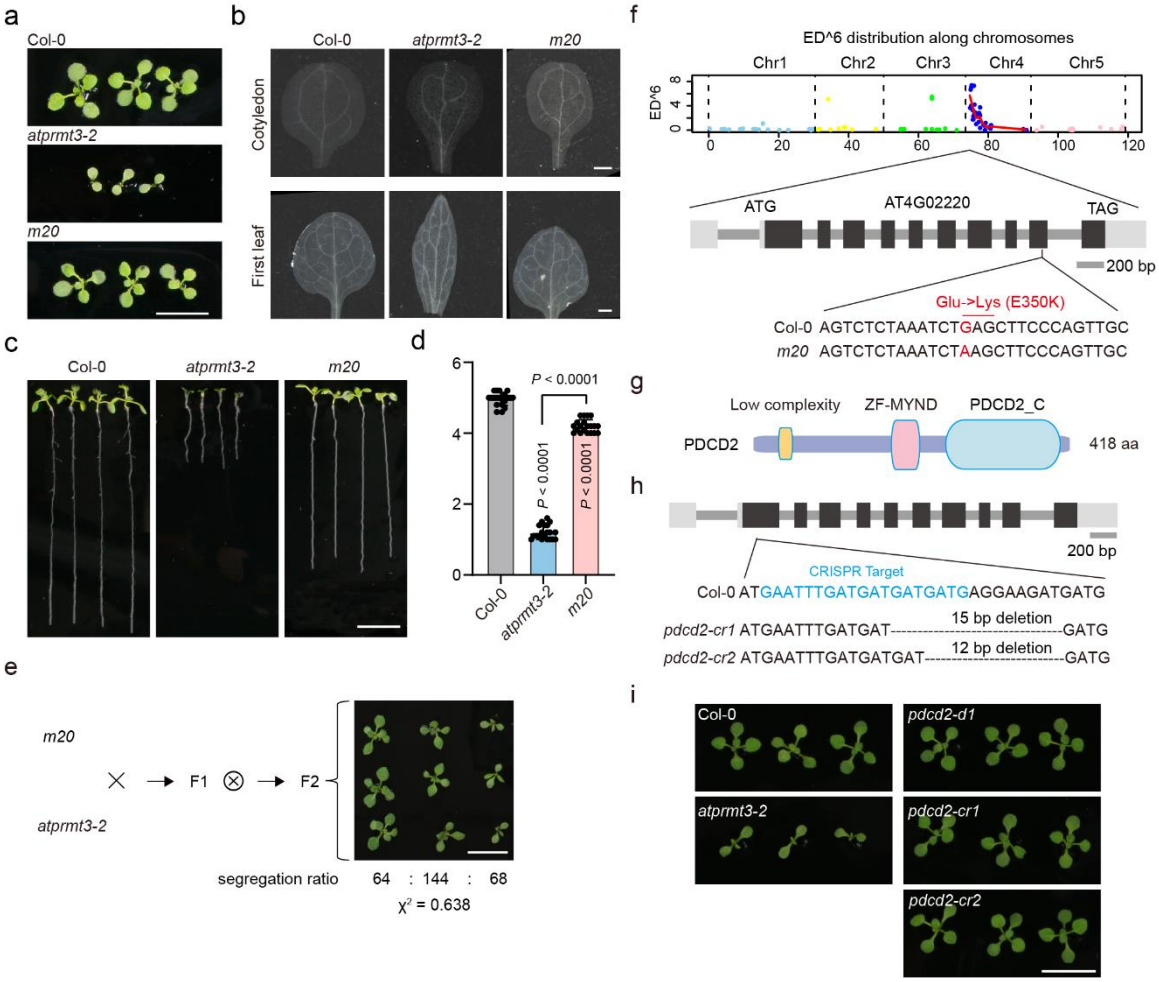

Supplementary Fig. 1. The suppressor *m20* partially rescues the pleiotropic developmental defects of *atprmt3-2* mutants. a Phenotypes of the aboveground seedlings. Ten-day-old seedlings of Col-0, *atprmt3-2*, and *m20* are shown. Scale bar, 1 cm. **b** Phenotypes of cotyledon and first true leaves. The cotyledon and first true leaves from twenty-day-old seedlings are shown. Scale bar, 500 μm. **c** Phenotypes of primary root length. Roots from ten-day-old seedlings are shown. Scale bar, 1 cm. **d** Quantitative measurement of root length in (**c**). Data are presented as mean values ± SD (n = 20). *P* value was calculated by One-way ANOVA with Dunnett's multiple comparisons test. **e** Genetic analysis of *m20* suppressor. *m20* was crossed with *atprmt3-2* to generate F1, F2 generation was generated by F1 self-fertilization, the phenotypes and genotypes in F2 were analyzed. Scale bar, 1 cm. **f** Genetic mapping of suppressor *m20*. The ED distribution along five chromosomes. Whole genome resequencing maps a G-to-A mutation in the 9th exon of *AT4G02220*. **g** Protein structure of PDCD2. The low complexity region, ZF-MYND,

and PDCD2_C domain are shown. **h** CRISPR-Cas9 to knockout *PDCD2*. The sequences in blue were shown as CRISPR target. A 15-bp and 12-bp deletion was identified in *pdcd2-cr1* and *pdcd2-cr2*, respectively. **i** Phenotypes of the aboveground seedlings. Ten-day-old seedlings of Col-0, *atprmt3-2*, *pdcd2-d1*, *pdcd2-cr1*, and *pdcd2-cr2* mutants are shown. Scale bar, 1 cm. Source data are provided as a Source Data file.

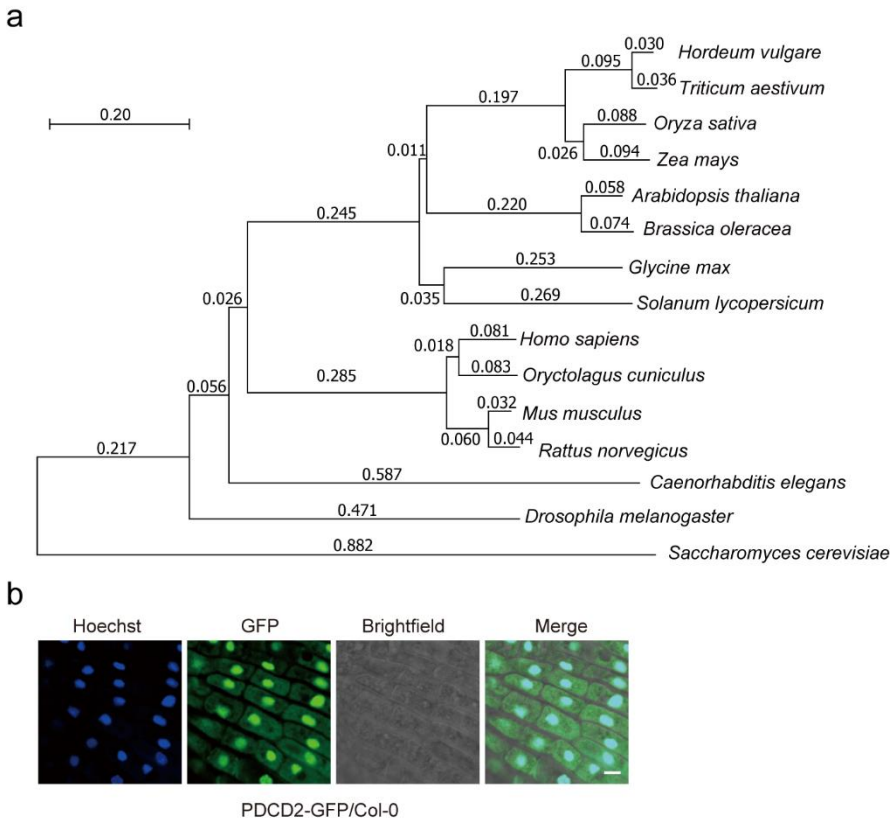

Supplementary Fig. 2. Characterization of PDCD2. a Phylogenic analysis of PDCD2 from different species. **b** PDCD2 is localized in both the nucleus and the cytoplasm. GFP fluorescence in root tissues of *PDCD2-GFP*/Col-0 were observed in green. Hoechst was stained for nuclear visualization in blue. Scale bar, 5 μm. Experiments were repeated two times with similar results.

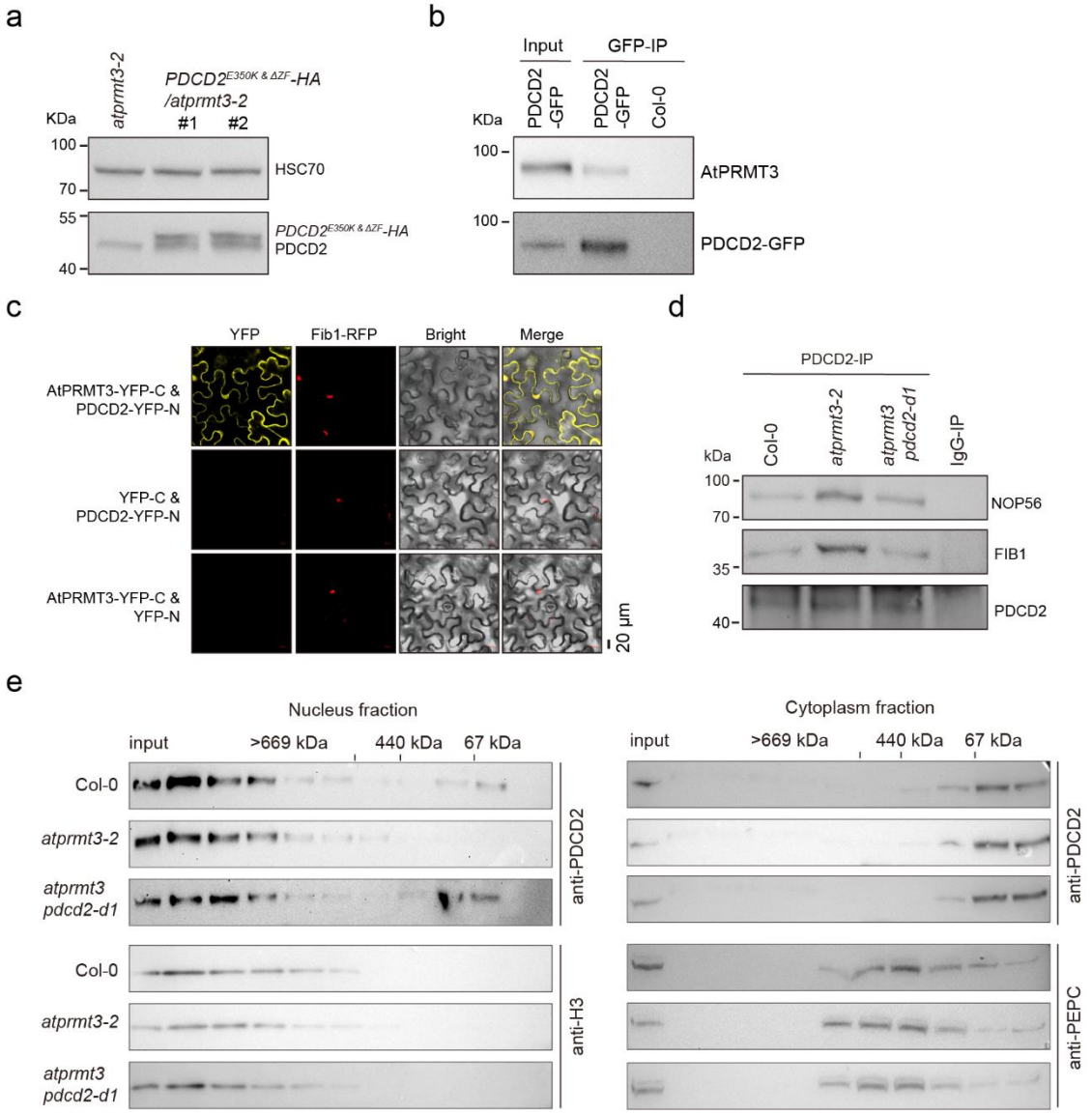

Supplementary Fig. 3. PDCD2 interacts with AtPRMT3 and pre-ribosome. a Immunoblotting detection for *PDCD2*$^{E350K\&\Delta ZF}$*-HA* transgenic plants. Total proteins were immunoblotted with anti-PDCD2, and anti-HSC70 antibodies. HSC70 was used as the control. **b** The interaction between AtPRMT3 and PDCD2 validated by co-immunoprecipitation. Proteins from *PDCD2-GFP* transgenic plants were immunoprecipitated by GFP-Trap beads, and immunoblotted by anti-AtPRMT3 and anti-GFP respectively. **c** The interaction between AtPRMT3 and PDCD2 validated by BiFC assay. Fib1-RFP was used as a nucleolus marker. **d** Immunoblotting results showing the associations between U3 snoRNP (NOP56 and FIB1) and PDCD2. Nuclear extracts from Col-0, *atprmt3-2*, and suppressor *atprmt3pdcd2-d1* were immunoprecipitated with anti-

PDCD2, IgG was used a negative control, and then immunoblotted with anti-NOP56, anti-FIB1, and anti-PDCD2 antibodies. **e** Gel filtration patterns of PDCD2/PDCD2^{E350K} in nucleus and cytoplasm fractions. Protein lysates from Col-0, *atprmt3-2*, and suppressor *atprmt3pdcd2-d1* were fractioned by gel filtration after subcellular fractionation, and immunoblotted with anti-PDCD2 antibody. PEPC (phosphoenolpyruvate carboxylase) and histone H3 were used as markers for cytoplasm and nucleus, respectively. All experiments were repeated at least two times with similar results. Source data are provided as a Source Data file.

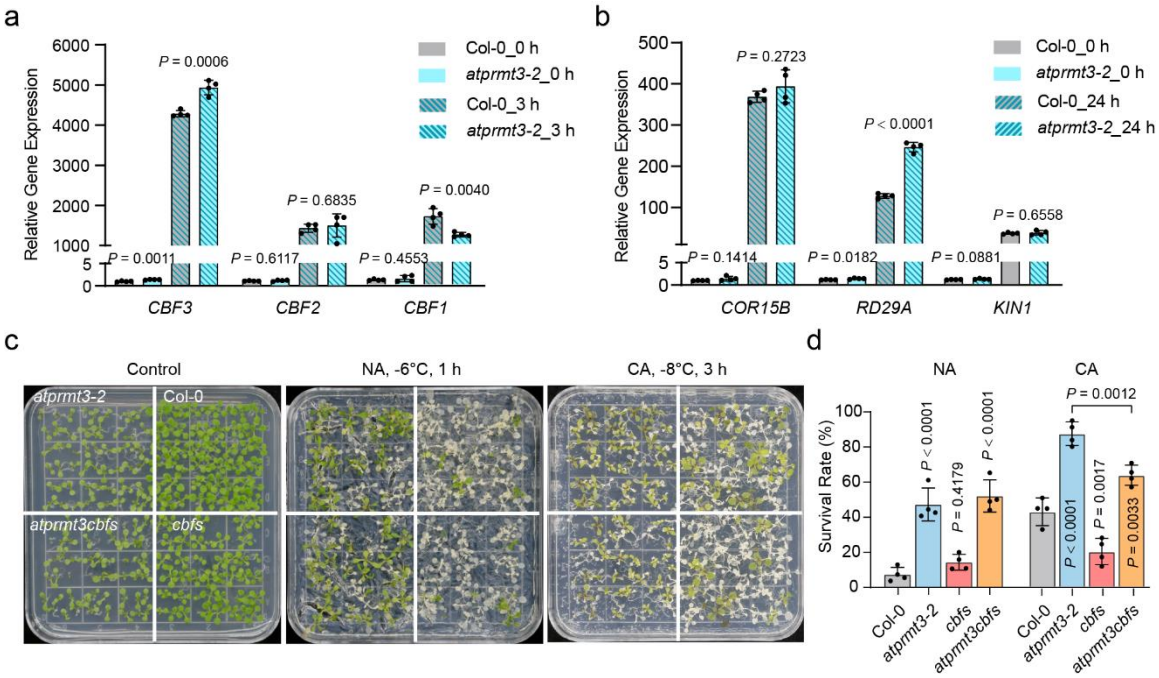

Supplementary Fig. 4. Freezing tolerance of *atprmt3-2* is partially dependent on CBF-pathway. a, b The expression patterns of *CBFs* (**a**) and *CORs* (**b**) in Col-0 and *atprmt3-2* under cold stress. Data are presented as mean values ± SD (n = 4). **c** Freezing phenotypes. Twelve-day-old seedlings of Col-0, *atprmt3-2*, *cbfs*, and *atprmt3cbfs* were subjected to freezing assay under NA and CA conditions. **d** The survival rates of plants in (**c**). Data are presented as mean values ± SD (n = 4). *P* value was calculated by One-way ANOVA with Dunnett's multiple comparisons test. Source data are provided as a Source Data file.

a

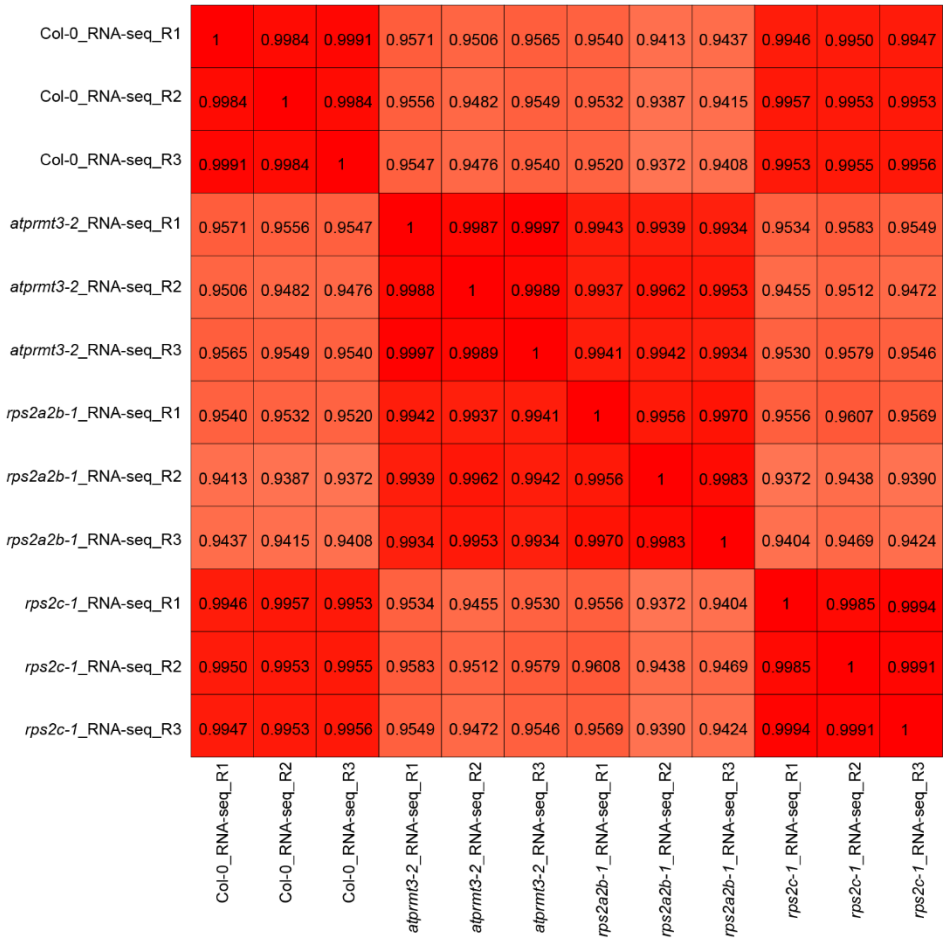
Col-0_RNA-seq_R1 1 0.9984 0.9991 0.9571 0.9506 0.9565 0.9540 0.9413 0.9437 0.9946 0.9950 0.9947
Col-0_RNA-seq_R2 0.9984 1 0.9984 0.9556 0.9482 0.9549 0.9532 0.9387 0.9415 0.9957 0.9953 0.9953
Col-0_RNA-seq_R3 0.9991 0.9984 1 0.9547 0.9476 0.9540 0.9520 0.9372 0.9408 0.9953 0.9955 0.9956
atprmt3-2_RNA-seq_R1 0.9571 0.9556 0.9547 1 0.9987 0.9997 0.9943 0.9939 0.9934 0.9534 0.9583 0.9549
atprmt3-2_RNA-seq_R2 0.9506 0.9482 0.9476 0.9988 1 0.9989 0.9937 0.9962 0.9953 0.9455 0.9512 0.9472
atprmt3-2_RNA-seq_R3 0.9565 0.9549 0.9540 0.9997 0.9989 1 0.9941 0.9942 0.9934 0.9530 0.9579 0.9546
rps2a2b-1_RNA-seq_R1 0.9540 0.9532 0.9520 0.9942 0.9937 0.9941 1 0.9956 0.9970 0.9556 0.9607 0.9569
rps2a2b-1_RNA-seq_R2 0.9413 0.9387 0.9372 0.9939 0.9962 0.9942 0.9956 1 0.9983 0.9372 0.9438 0.9390
rps2a2b-1_RNA-seq_R3 0.9437 0.9415 0.9408 0.9934 0.9953 0.9934 0.9970 0.9983 1 0.9404 0.9469 0.9424
rps2c-1_RNA-seq_R1 0.9946 0.9957 0.9953 0.9534 0.9455 0.9530 0.9556 0.9372 0.9404 1 0.9985 0.9994
rps2c-1_RNA-seq_R2 0.9950 0.9953 0.9955 0.9583 0.9512 0.9579 0.9608 0.9438 0.9469 0.9985 1 0.9991
rps2c-1_RNA-seq_R3 0.9947 0.9953 0.9956 0.9549 0.9472 0.9546 0.9569 0.9390 0.9424 0.9994 0.9991 1
Col-0_RNA-seq_R1
Col-0_RNA-seq_R2
Col-0_RNA-seq_R3
atprmt3-2_RNA-seq_R1
atprmt3-2_RNA-seq_R2
atprmt3-2_RNA-seq_R3
rps2a2b-1_RNA-seq_R1
rps2a2b-1_RNA-seq_R2
rps2a2b-1_RNA-seq_R3
rps2c-1_RNA-seq_R1
rps2c-1_RNA-seq_R2
rps2c-1_RNA-seq_R3

b

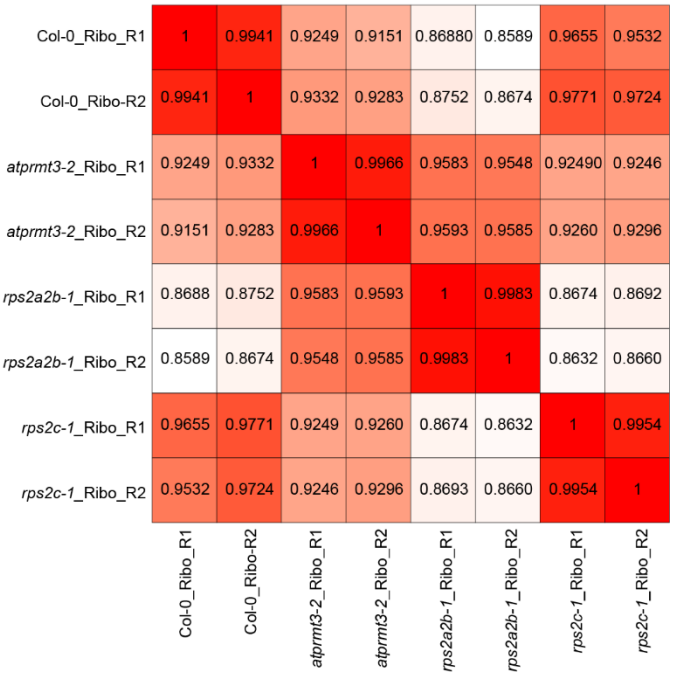
Col-0_Ribo_R1 1 0.9941 0.9249 0.9151 0.86880 0.8589 0.9655 0.9532
Col-0_Ribo-R2 0.9941 1 0.9332 0.9283 0.8752 0.8674 0.9771 0.9724
atprmt3-2_Ribo_R1 0.9249 0.9332 1 0.9966 0.9583 0.9548 0.92490 0.9246
atprmt3-2_Ribo_R2 0.9151 0.9283 0.9966 1 0.9593 0.9585 0.9260 0.9296
rps2a2b-1_Ribo_R1 0.8688 0.8752 0.9583 0.9593 1 0.9983 0.8674 0.8692
rps2a2b-1_Ribo_R2 0.8589 0.8674 0.9548 0.9585 0.9983 1 0.8632 0.8660
rps2c-1_Ribo_R1 0.9655 0.9771 0.9249 0.9260 0.8674 0.8632 1 0.9954
rps2c-1_Ribo_R2 0.9532 0.9724 0.9246 0.9296 0.8693 0.8660 0.9954 1
Col-0_Ribo_R1
Col-0_Ribo-R2
atprmt3-2_Ribo_R1
atprmt3-2_Ribo_R2
rps2a2b-1_Ribo_R1
rps2a2b-1_Ribo_R2
rps2c-1_Ribo_R1
rps2c-1_Ribo_R2

Supplementary Fig. 5. Reproducibility of RNA-seq and Ribo-seq libraries. Correlation of the biological replicates for RNA-seq (**a**), and Ribo-seq (**b**).

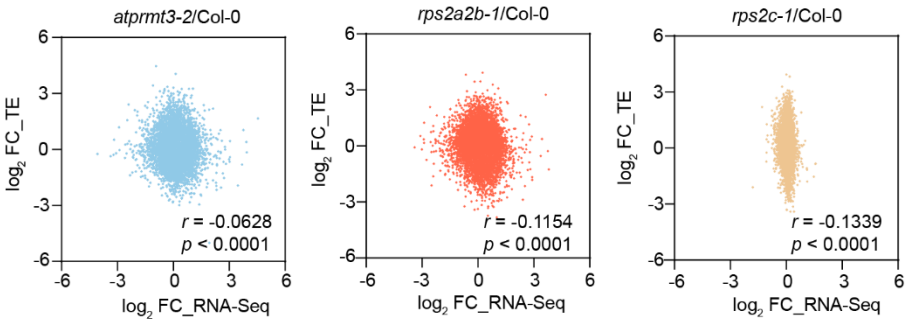

Supplementary Fig. 6. The relationship between TE and transcriptional changes. Scatter plots comparing fold-changes (FC) of FPKM between RNA-seq (*x*-axis) and TE (*y*-axis). Pearson *r* and *p* value (two-tailed) are shown.

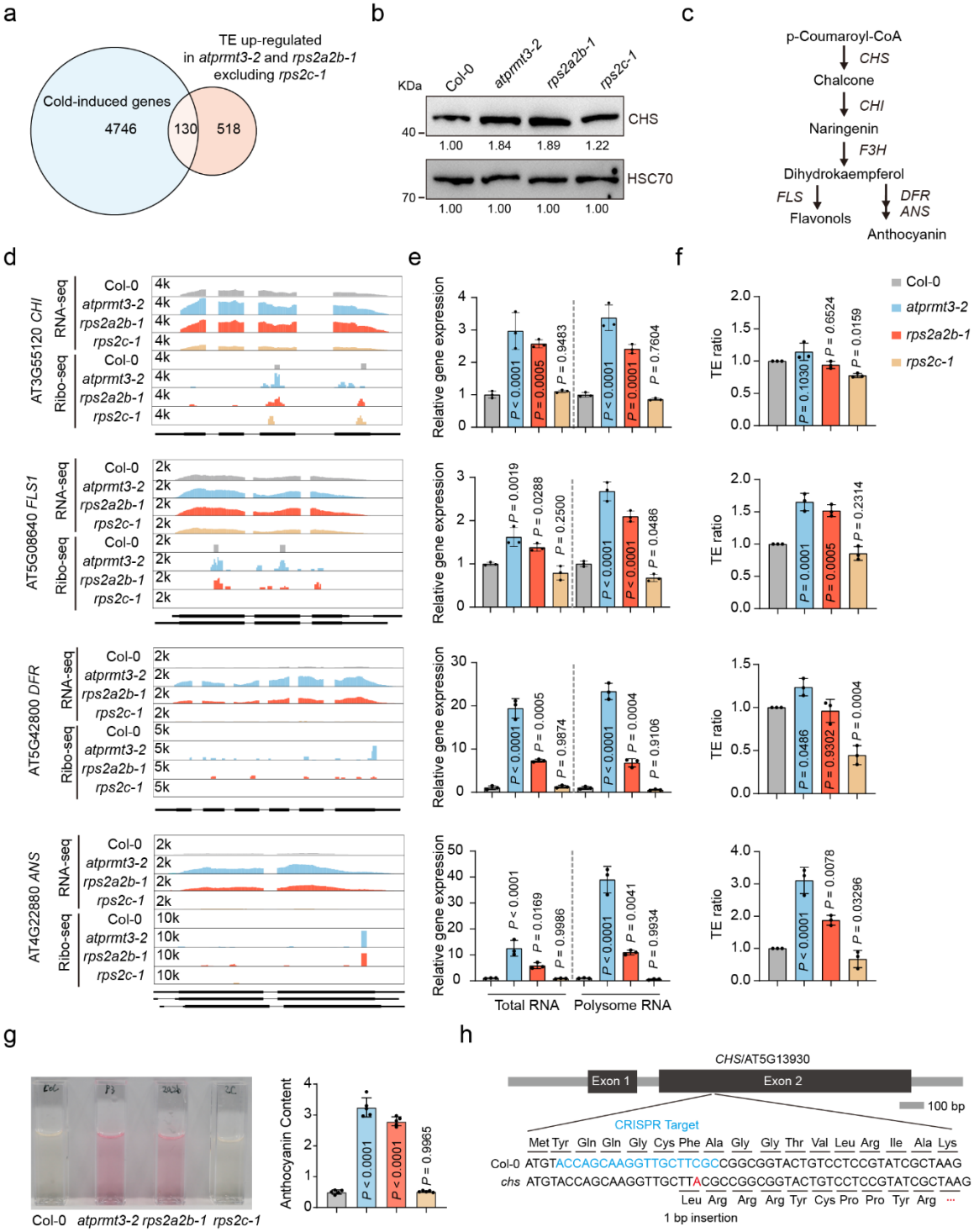

Supplementary Fig. 7. AtPRMT3-RPS2 co-regulates gene expression involved in flavonoid pathway. a Venn diagrams showing the overlap between cold induced genes and TE upregulated genes in *atprmt3-2* and *rps2a2b-1* excluding *rps2c-1*. **b** The protein levels of CHS. Total proteins were immunoblotted with anti-CHS and anti-HSC70

antibodies. HSC70 was used as the control. Experiments were repeated three times with similar results. **c** A simplified schematic representation of flavonoid pathways. **d** Representative genome browser view of RNA-seq and Ribo-seq for *CHI*, *FLS1*, *ANS*, and *DFR*. **e** Expression validation for *CHI*, *FLS1*, *ANS*, and *DFR*. Toal RNA and polysome-bound RNA from Col-0, *atprmt3-2*, *rps2a2b-1*, and *rps2c-1* were used for qRT-PCR. Data are presented as mean values ± SD (n = 3). **f** Translation efficiency (TE) analysis in (**e**). Data are presented as mean values ± SD (n = 3). **g** Anthocyanin content. Data are presented as mean values ± SD (n = 5). **h** CRISPR-Cas9 to knockout *CHS*. The sequences in blue were shown as CRISPR target, a single base A (shown in red) was inserted in *chs* mutant, which causes a premature stop codon. *P* value was calculated by One-way ANOVA with Dunnett's multiple comparisons test. Source data are provided as a Source Data file.

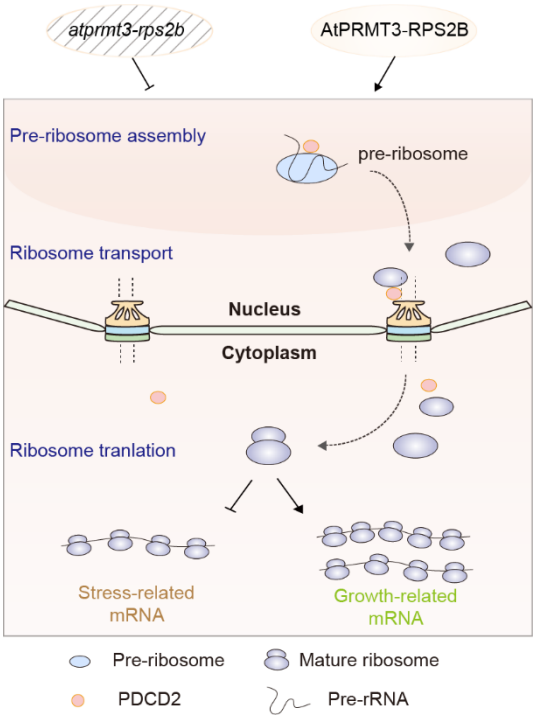

Supplementary Fig. 8. Working model of AtPRMT3-RPS2-PDCD2 in regulating ribosome biogenesis and translation. In wild type, AtPRMT3-RPS2B plays a crucial role in facilitating the accurate pre-ribosome assembly in nucleus. PDCD2 could interact with pre-ribosome, and facilitate their efficient export to cytoplasm. Once in cytoplasm, functional ribosomes actively contribute to the translation of genes associated with growth, simultaneously suppressing the translation of genes related to stress. However, the disruption of AtPRMT3-RPS2B could lead to aberrant pre-ribosome assembly in nucleus, ultimately result in abnormal ribosome translation in cytoplasm, which disturb the translational balance between stress and growth-related genes.

Supplementary Table 1. PDCD2-associated proteins in nucleus identified by IP-MS

		PDCD2-IP		IgG-IP
Name	ID	All peptides	Unique peptides	All peptides
PDCD2	AT4G02220	20	20	0
RPS2B	AT1G59359; AT1G58983; AT1G58684	10	3	0
RPS2C	AT2G41840	11	4	3
FIB1	AT5G52470	8	2	0
FIB2	AT4G25630	7	1	0
NOP56	AT1G56110	3	3	0
NOP58	AT3G05060	2	2	0
GP210	AT5G40480	7	7	0
XPO1A	AT5G17020	6	6	0
LOS4	AT3G53110	5	5	0
NUP155	AT1G14850	5	5	0
NUP85	AT4G32910	4	4	0
NUP93A	AT2G41620	4	4	0
DUF3414	AT5G51200	4	4	0
HOS1	AT2G39810	2	2	0
NUP35	AT3G16310	2	2	0
NUP133	AT2G05120	2	2	0
NUP96	AT1G80680	1	1	0
NUP160	AT1G33410	1	1	0
NUP107	AT3G14120	1	1	0
NUP214	AT1G55540	1	1	0

Supplementary Table 2. Primers used in this study.

Primer ID	Sequence (5'->3')	Application
HX3425	GCATGTCTCAACTTCGCTGA	*CBF1*, qRT-PCR, F
HX3426	ATCGTCTCCTCCATGTCCAG	*CBF1*, qRT-PCR, R
HX3427	TGACGTGTCCTTATGGAGCTA	*CBF2*, qRT-PCR, F
HX3428	CTGCACTCAAAAACATTTGCA	*CBF2*, qRT-PCR, R
HX3429	GATGACGACGTATCGTTATGGA	*CBF3*, qRT-PCR, F
HX3430	TACACTCGTTTCTCAGTTTTACAAAC	*CBF3*, qRT-PCR, R
HX3431	GCCGAGAAACTTCAGATTGG	*RD29A*, qRT-PCR, F
HX3432	CCATTCCTCCTCCTCCTTTC	*RD29A*, qRT-PCR, R
HX3433	AAAGCAGAGTGGTGTTGGTACCGT	*COR15b*, qRT-PCR, F
HX3434	TCATCGAGGATGTTGCCGTCACTT	*COR15b*, qRT-PCR, R
HX3437	ACCAACAAGAATGCCTTCCA	*KIN1*, qRT-PCR, F
HX3438	CCGCATCCGATACACTCTTT	*KIN1*, qRT-PCR, R
CP2466	TCAAGCGCATGTGCGACAAGTCGA	*CHS*, qRT-PCR, F
CP2467	TTGGTGAGCTGGTAGTCAGCACCA	*CHS*, qRT-PCR, R
CP2468	AAATAGTCACCGGTGCGTTTGAGA	*CHI*, qRT-PCR, F
CP2469	CGTAAGAGAGCCGGTAGGGGAGAG	*CHI*, qRT-PCR, R
CP2474	AAAGATCCTGAGAACGAAGTGATA	*DFR*, qRT-PCR, F
CP2475	CCATCCTGTCATCTTTTTGGACAT	*DFR*, qRT-PCR, R
CP2476	AAGTGATTACATAGAAGCAACGAG	*ANS*, qRT-PCR, F
CP2477	GGTGTGAGCTTCCACACCGAGTGC	*ANS*, qRT-PCR, R
CP2478	GATCAGATTCTGAGGTTGAGTAAT	*FLS1*, qRT-PCR, F
CP2479	ATCCAGAGGAAGTTTATTGAGCTT	*FLS1*, qRT-PCR, R
CF6127	ACGGCCACTATGTTTGTTGCGGGA	*AtPRMT3*, qRT-PCR, F
CF6128	CAGGTCAAATGTCTGAAGAAGGGT	*AtPRMT3*, qRT-PCR, F
CP0420	GTGGTGTTCCGGCATGGTTGGA	*PDCD2*, qRT-PCR, F
CP0421	AAAACCTTCGTACTCCGCATAG	*PDCD2*, qRT-PCR, F
WZ022	GTCGTACAACCGGTATTGTGCTGG	*ACTIN2*, qRT-PCR, F
WZ023	CCATCTCCTGCTCGTAGTCAACAG	*ACTIN2*, qRT-PCR, R
CX9204	CCATTCAAGCCTCCTAAGGTGG	*UBQ10*, qRT-PCR, F
CX9205	CGATAGCAGCACCTTGGAAATGG	*UBQ10*, qRT-PCR, R
CP1280	ATTGACCAGCAAGGTTGCTTCGC	*CHS*, CRISPR
CP1281	AAACGCGAAGCAACCTTGCTGGT	*CHS*, CRISPR
CP6895	TTTTCTGATTAACAGAATTCATGAGTAGCTTCAACGGAGA	*PDCD2*, F
CP6896	GCTAACCGTTCGAAGCTGTTGAAGCGGAGCTCCATGACCCAA	*PDCD2*-ΔZF, F
CP6897	TTGGGTCATGGAGCTCCGCTTCAACAGCTTCGAACGGTTAGC	*PDCD2*-ΔZF, R
CP6898	TCTCCATGGTCTAGAGGATCCAGTTGTCTGACTGTATAGTTG	*PDCD2*, R
CP1796	CCATGGAGGCCAGTGAATTCATGAGTAGCTTCAACGGAGA	*PDCD2-AD*, F
CP1797	AGCTCGAGCTCGATGGATCCCTAAGTTGTCTGACTGTATA	*PDCD2-AD*, R
HX6500	TCCCCCCGGGATGGCGGAAAGAGGAGGAG	*RPS2B-BD*, F
HX6505	GGAATTCAGCTTGGTCTTCACCCTC	*RPS2B-BD*, R
CP1145	GCGTCCCGGGGCGGTACCATGAGTAGCTTCAACGGA	*cLUC-PDCD2*, F

CP1146	GTAGTCCATTTGTTGGATCCCTAAGTTGTCTGACTGTA	*cLUC-PDCD2*, R
CP1155	GGGGACGAGCTCGGTACCATGGCGGAAAGAGGAGGAGA	*nLUC-RPS2B*, F
CP1156	GCGTACGAGATCTGGTCGACAGCTTGGTCTTCACCCTCAG	*nLUC-RPS2B*, R
CP1153	GGGGACGAGCTCGGTACCATGGCGGCGACAATGGTG	*nLUC-AtPRMT3*, F
CP1154	GCGTACGAGATCTGGTCGACTAGATTAAATATCTGAAC	*nLUC-AtPRMT3*, R
XP1061	TGGCGCGCCACTAGTGGATCCATGGCGGCGACAATGGTGAAG	*AtPRMT3-YCE*, F
XP1062	CCCGGGAGCGGTACCCTCGAGTAGATTAAATATCTGAACCGG	*AtPRMT3-YCE*, R
XP1065	TGGCGCGCCACTAGTGGATCCATGAGTAGCTTCAACGGAGAC	*PDCD2-YNE*, F
XP1066	CCCGGGAGCGGTACCCTCGAGAGTTGTCTGACTGTATAGTTG	*PDCD2-YNE*, R
HX2540	Cy3-GTCGTTCTGTTTTGGACAGGTATCGA	RNA FISH